Meson spectroscopy at the Tevatron

Kai Yi for the CDF and D0 Collaboration

Department of Physics and Astronomy, University of Iowa, Iowa City, IA 52242, USA

Abstract. The Tevatron experiments have each accumulated about 6 fb^{-1} good data since the start of RUN II. This large dataset provided good opportunities for meson spectroscopy studies at the Tevatron. This article will cover the recent new $\Upsilon(nS)$ polarization studies as well as exotic meson spectroscopy studies.

Keywords: meson, exotic, spectroscopy
PACS: 14.40.Nd, 14.40.Lb, 14.40.Pq

$\Upsilon(nS)$ **POLARIZATION**

Vector meson production and polarization in hadronic collisions is usually discussed within the framework of non-relativistic QCD (NRQCD). The theory predicts [1] that the vector meson polarization should become transverse in the perturbative regime; *i.e.*, at large transverse momentum p_T of the vector meson. However, the prediction is not supported by experimental observations [2]. We describe new results on this topic from the Tevatron. We define a parameter–α to measure the polarization:

$$\frac{d\Gamma}{dcos\theta^*} \propto 1 + \alpha cos^2\theta^* \tag{1}$$

where θ^* is the μ^+ angle in the rest frame of $\Upsilon(nS)$ with respect to the $\Upsilon(nS)$ direction in the lab frame. If the meson is fully polarized in the transverse direction, $\alpha = 1$. If it is fully aligned longitudinally, $\alpha = -1$.

Fig. 1 shows the comparison between the theoretical prediction of $\Upsilon(1S)$ (colored band) and the new CDF (left) [3] and D0 (right) [4] experimental results. In the low p_T region, CDF shows nearly-unpolarized events, which is consistent with the CDF Run I result [5]; D0 shows partially longitudinally polarized events. At higher p_T, the CDF results tend toward longitudinal polarization while the D0 result indicates transverse polarization. Both CDF and D0 results at high p_T deviate from theoretical predictions. It will be interesting to investigate it with more data and in some detail; *e.g.* study η dependence since CDF and D0 have different η acceptance.
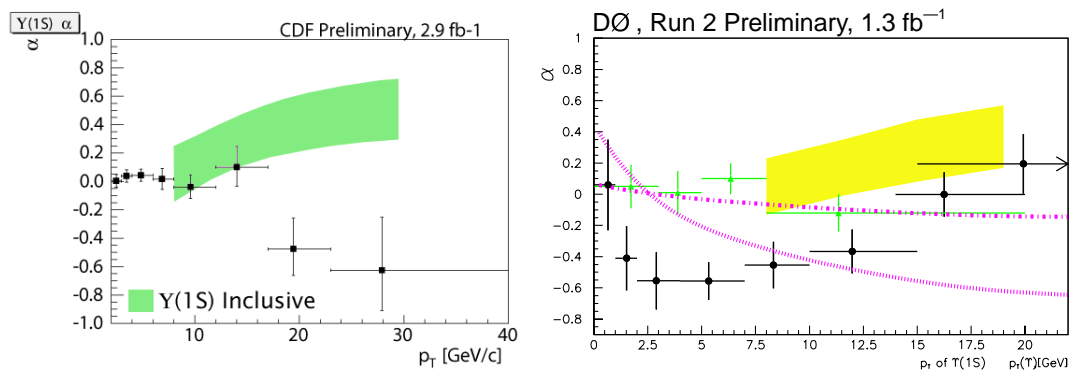

FIGURE 1. The polarization parameter α of $\Upsilon(1S)$ measured by CDF (left) and D0 (right, CDF I results were shown as green points).

EXOTIC MESONS

It has been six years since the discovery of the $X(3872)$ [6]; however, the nature of this state has not yet been clearly understood. Due to the proximity of the $X(3872)$ to the D^0D^{*0} threshold, the $X(3872)$ has been proposed as a molecule

composed of D^0 and D^{*0} mesons. The $X(3872)$ has also been speculated to be two nearby states, as in models such as the *diquark − antidiqurk* model. It is critical to make precise measurements of the mass and width of $X(3872)$ to understand its nature. The large $X(3872) \to J/\psi\pi^+\pi^-$ sample accumulated at CDF enables a test of the hypothesis that the $X(3872)$ is composed of two states and to make a precise mass measurement of $X(3872)$ if it is consistent with a one-state hypothesis.

There are many more states, similar to $X(3872)$, that have charmonium-like decay modes but are difficult to place in the overall charmonium system [7, 8, 9]. These unexpected new states have introduced challenges to the conventional $q\bar{q}$ meson model and revitalized interest in exotic mesons in the charm sector [10], although the existence of exotic mesons has been discussed for many years [11]. Until recently all of these new states involved only c quark and light quark (u, d) decay products. The $J/\psi\phi$ final state enables us to extend the exotic meson searches to c quark and heavy s quark decay products. An investigation of the $J/\psi\phi$ system produced in exclusive $B^+ \to J/\psi\phi K^+$ decays with $J/\psi \to \mu^+\mu^-$ and $\phi \to K^+K^-$ is reported here. Charge conjugate modes are included implicitly in this note.
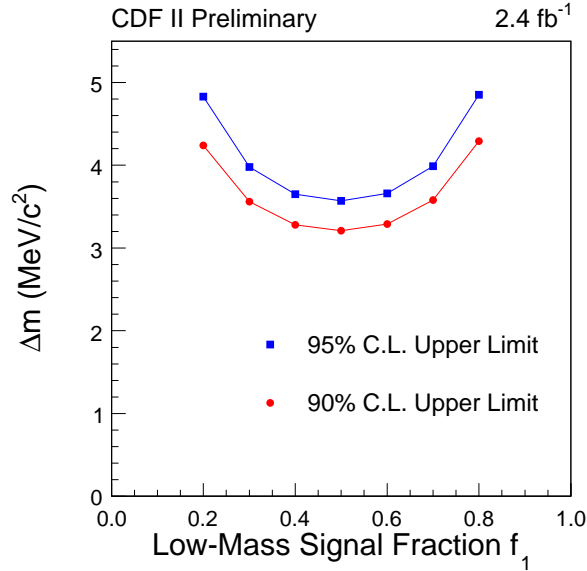
Measurement of the mass of $X(3872)$

FIGURE 2. The dependence of the upper limit on the mass difference Δm between two states on the low-mass state signal fraction f_1.

We tested the hypothesis of whether the observed X(3872) signal is composed of two different states as predicted in some four-quark models using the CDF inclusive $X(3872)$ sample. We fit the $X(3872)$ mass signal with a Breit-Wigner function convoluted with a resolution function [12]. Both functions contain a width scale factor that is a free parameter in the fit and therefore sensitive to the shape of the mass signal. The measured width scale factor is compared to the values seen in simulations which assume two states with the given mass difference and ratio of events. The resolution in the simulated events is corrected for the difference between data and simulation as measured from the $\psi(2S)$. The result of this hypotheses test shows that the data is consistent with a single state. Under the assumption of two states with equal amount of observed events, we set a limit of $\Delta m < 3.2(3.6)$ MeV/c^2 at 90% (95%) C.L. The limit for other ratios of events in the two peaks is shown in Fig. 2.

Since the $X(3872)$ is consistent with one peak in our test, we proceed to measure its mass in an unbinned maximum likelihood fit. The systematic uncertainties are determined from the difference between the measured $\psi(2S)$ mass and its world average value, the potential variation of the $\psi(2S)$ mass as a function of kinematic variables, and the difference in Q value between $X(3872)$ and $\psi(2S)$. Systematics due to the fit model are negligible. The measured $X(3872)$ mass is: $m(X(3872)) = 3871.61 \pm 0.16(stat) \pm 0.19(syst)$ MeV/c^2, which is the most precise measurement to date, as shown in Fig. 3 [12, 13].
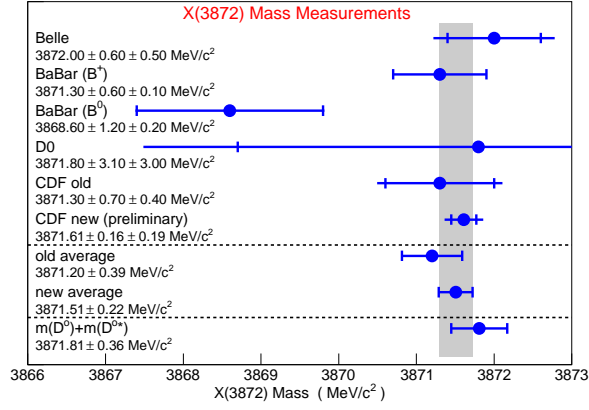
FIGURE 3. An overview of the measured $X(3872)$ masses from the experiments observing the $X(3872)$.
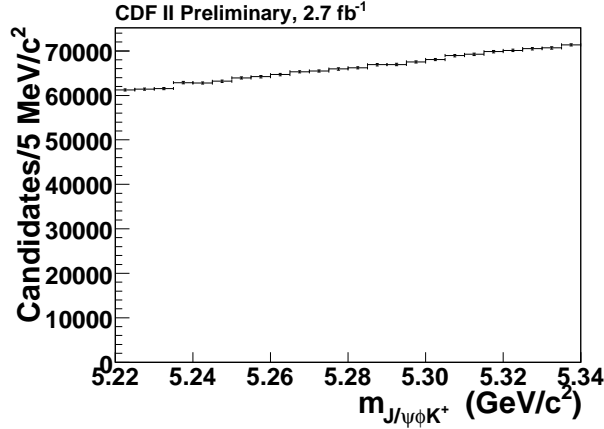
Evidence for Y(4140)

FIGURE 4. The $J/\psi\phi K^+$ mass before minimum $L_{xy}(B^+)$ and kaon *LLR* requirements.

We first reconstruct the $B^+ \rightarrow J/\psi\phi K^+$ signal and then search for structures in the $J/\psi\phi$ mass spectrum [14]. The $J/\psi \rightarrow \mu^+\mu^-$ events are recorded using a dedicated dimuon trigger. The $B^+ \rightarrow J/\psi\phi K^+$ candidates are reconstructed by combining a $J/\psi \rightarrow \mu^+\mu^-$ candidate, a $\phi \rightarrow K^+K^-$ candidate, and an additional charged track. Each track is required to have at least 4 axial silicon hits and have a transverse momentum greater than 400 MeV/c. The reconstructed mass of each vector meson candidate must lie within a suitable range from the nominal values (± 50 MeV/c^2 for the J/ψ and ± 7 MeV/c^2 for the ϕ). In the final B^+ reconstruction the J/ψ is mass constrained, and the B^+ candidates must have $p_T > 4$ GeV/c. The $P(\chi^2)$ of the mass- and vertex-constrained fit to the $B^+ \rightarrow J/\psi\phi K^+$ candidate is required to be greater than 1%.

To suppress combinatorial background, we use dE/dx and Time-of-Flight (TOF) information to identify all three kaons in the final state. The information is summarized in a log-likelihood ratio (*LLR*), which reflects how well a candidate track can be positively identified as a kaon relative to other hadrons. In addition, we require a minimum $L_{xy}(B^+)$ for the $B^+ \rightarrow J/\psi\phi K^+$ candidate, where $L_{xy}(B^+)$ is the projection onto $\vec{p}_T(B^+)$ of the vector connecting the primary vertex to the B^+ decay vertex. The $L_{xy}(B^+)$ and *LLR* requirements for $B^+ \rightarrow J/\psi\phi K^+$ are then chosen to maximize $S/\sqrt{S+B}$, where S is the number of $B^+ \rightarrow J/\psi\phi K^+$ signal events and B is the number of background events implied from the B^+ sideband. The requirements obtained by maximizing $S/\sqrt{S+B}$ are $L_{xy}(B^+) > 500~\mu$m and $LLR > 0.2$.

The invariant mass of $J/\psi\phi K^+$, after J/ψ and ϕ mass window requirements, before and after the minimum $L_{xy}(B^+)$
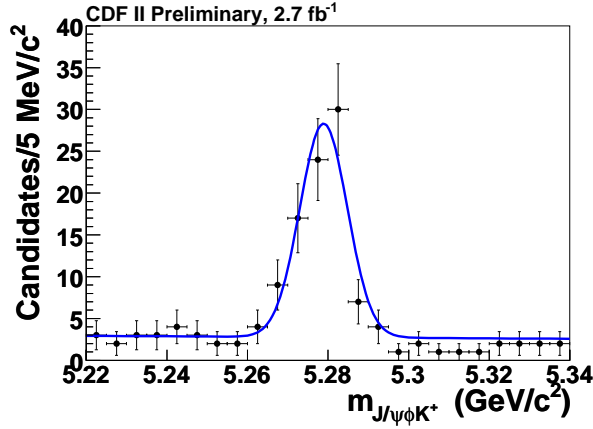
FIGURE 5. The $J/\psi\phi K^+$ mass after minimum $L_{xy}(B^+)$ and *LLR* requirements; the solid line is a fit to the data with a Gaussian signal function and linear background function.
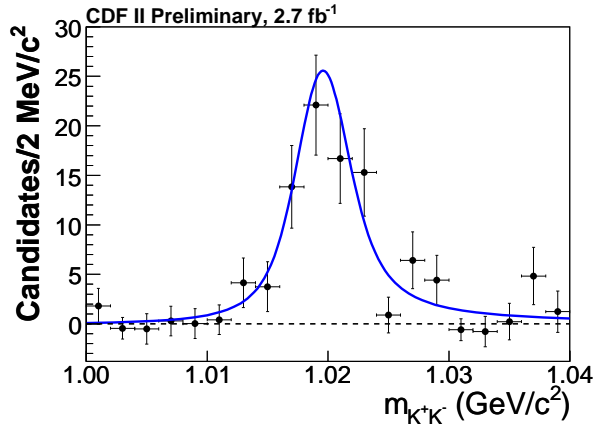

FIGURE 6. The B^+ sideband-subtracted K^+K^- mass without the ϕ mass window requirement. The solid curve is a *P*-wave relativistic Breit-Wigner fit to the data.

and kaon *LLR* requirements, are shown in Fig. 4 and Fig. 5, respectively. We do not distinguish the B^+ signal at all before the $L_{xy}(B^+)$ and kaon *LLR* requirements, but we see a clear B^+ signal after the requirements. A fit with a Gaussian signal function and a linear background function to the mass spectrum of $J/\psi\phi K^+$ (Fig. 5) returns a B^+ signal of $75 \pm 10(\text{stat})$ events. The $L_{xy}(B^+)$ and *LLR* requirements reduce the background by a factor of approximately 20 000 while keeping a signal efficiency of approximately 20%. We select B^+ signal candidates with a mass within 3σ of the nominal B^+ mass; the purity of the B^+ signal in that mass window is about 80%.

The combinatorial background under the B^+ peak includes B hadron decays such as $B_s^0 \to \psi(2S)\phi \to J/\psi\pi^+\pi^-\phi$, in which the pions are misidentified as kaons. However, background events with misidentified kaons cannot yield a Gaussian peak at the B^+ mass consistent with the 5.9 MeV/c^2 mass resolution. Figure 6 shows the K^+K^- mass from $\mu^+\mu^-K^+K^-K^+$ candidates within $\pm3\sigma$ of the nominal B^+ mass with B sidebands subtracted before applying the ϕ mass window requirement. Using a smeared *P*-wave relativistic Breit-Wigner (BW) [15] line-shape fit to the spectrum returns a χ^2 probability of 28%. This shows that the $B^+ \to J/\psi K^+K^-K^+$ final state is well described by $J/\psi\phi K^+$.

We then examine the effects of detector acceptance and selection requirements using $B^+ \to J/\psi\phi K^+$ MC events simulated by a phase space distribution. The MC events are smoothly distributed in the Dalitz plot and in the $J/\psi\phi$ mass spectrum. No artifacts were observed from MC events. Figure 7 shows the Dalitz plot of $m^2(\phi K^+)$ versus $m^2(J/\psi\phi)$, and Fig. 8 shows the mass difference, $\Delta M = m(\mu^+\mu^-K^+K^-) - m(\mu^+\mu^-)$, for events in the B^+ mass window in our data sample. We examine the enhancement in the ΔM spectrum just above $J/\psi\phi$ threshold. We exclude the high–mass part of the spectrum beyond 1.56 GeV/c^2 to avoid combinatorial backgrounds that would be expected
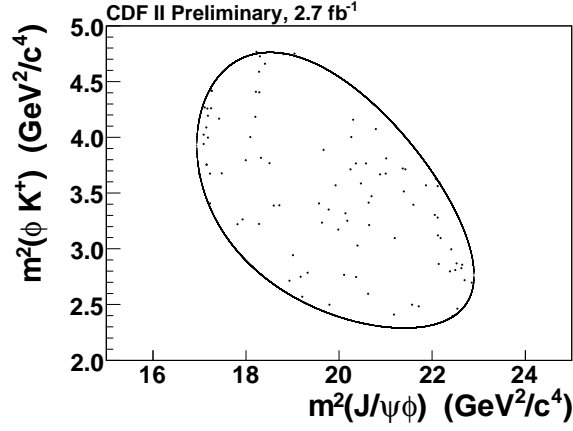
FIGURE 7. The Dalitz plot of $m^2(\phi K^+)$ versus $m^2(J/\psi\phi)$ in the B^+ mass window. The boundary shows the kinematically allowed region.
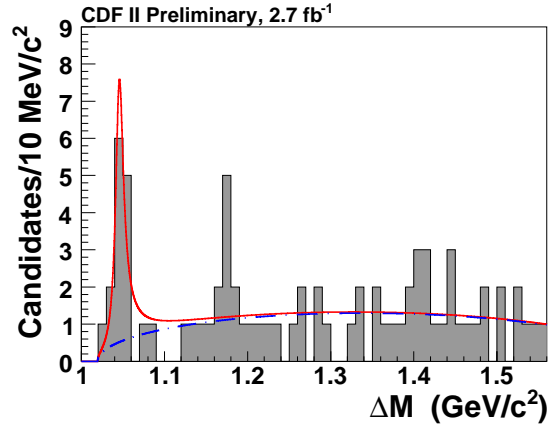

FIGURE 8. The mass difference, ΔM, between $\mu^+\mu^- K^+ K^-$ and $\mu^+\mu^-$, in the B^+ mass window. The dash-dotted curve is the background contribution and the red solid curve is the total unbinned fit.

from misidentified $B_s^0 \to \psi(2S)\phi \to (J/\psi\pi^+\pi^-)\phi$ decays. We model the enhancement by an S-wave relativistic BW function [16] convoluted with a Gaussian resolution function with the RMS fixed to 1.7 MeV/c^2 obtained from MC, and use three–body phase space [11] to describe the background shape. An unbinned likelihood fit to the ΔM distribution, as shown in Fig. 8, returns a yield of 14 ± 5 events, a ΔM of 1046.3 ± 2.9 MeV/c^2, and a width of $11.7^{+8.3}_{-5.0}$ MeV/c^2. To investigate possible reflections, we examine the Dalitz plot and projections into ϕK^+ and $J/\psi K^+$ spectrum. We find no evidence for any other structure in the ϕK^+ and $J/\psi K^+$ spectrum.

We use the log-likelihood ratio of $-2\ln(\mathcal{L}_0/\mathcal{L}_{max})$ to determine the significance of the enhancement, where $\mathcal{L}_0$ and $\mathcal{L}_{max}$ are the likelihood values for the null hypothesis fit and signal hypothesis fit. The $\sqrt{-2\ln(\mathcal{L}_0/\mathcal{L}_{max})}$ value is 5.3 for a pure three–body phase space background shape assumption. We generate ΔM spectra using the background distribution alone, and search for the most significant fluctuation with $\sqrt{-2\ln(\mathcal{L}_0/\mathcal{L}_{max})} \geq 5.3$ in each spectrum in the mass range of 1.02 to 1.56 GeV/c^2, with widths in the range of 1.7 (detector resolution) to 120 MeV/c^2 (ten times the observed width).

The resulting p-value from 3.1 million simulations is 9.3×10^{-6}, corresponding to a significance of 4.3σ. We repeat this process with a flat combinatorial non-B background and three–body PS for non-resonance B background and we still get a significance of 3.8σ.

One's eye tends to be drawn to a second cluster of events around 1.18 GeV/c^2 in Fig. 8, or around 4.28 GeV/c^2 in $J/\psi\phi$ mass as shown in Fig. 9. This cluster is close to one pion mass above the peak at the $J/\psi\phi$ threshold. However,
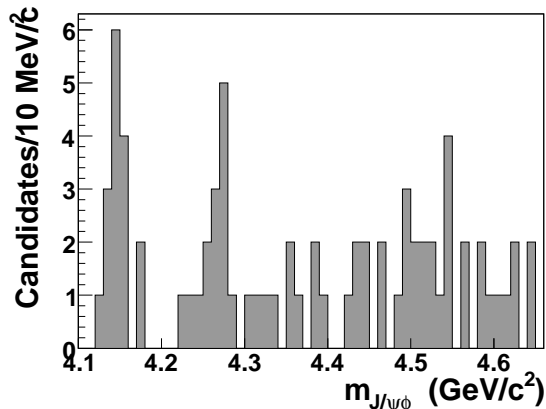
FIGURE 9. The $J/\psi\phi$ mass distribution in the B^+ mass window.

this cluster is statistically insufficient to infer the presence of a second structure.

SUMMARY

For $\Upsilon(1S)$ polarization, CDF result shows nearly-unpolarized events at low p_T, while D0 shows partially longitudinally polarized. At higher p_T, CDF results tend toward longitudinal polarization while D0 result shows transverse polarization. Both CDF and D0 results at high p_T deviate from theoretical predictions. CDF is continuing the analysis and will double the dataset. D0 has the opportunity to study the rapidity dependence, since their measurement spans the range $|y| < 1.8$ compared to 0.6 for CDF.

Studies using CDF's $X(3872)$ sample, the largest in the world, indicate that the $X(3872)$ is consistent with the one state hypothesis and this leads to the most precise mass measurement of ($X3872$). The value is below, but within the uncertainties of the $D^{*0}D^0$ threshold. The explanation of the X(3872) as a bound D*D system is therefore still an option.

The $B^+ \rightarrow J/\psi\phi K^+$ sample at CDF enables us to search for structure in the $J/\psi\phi$ mass spectrum, and we find evidence for a narrow structure near the $J/\psi\phi$ threshold with a significance estimated to be at least 3.8σ. Assuming an S-wave relativistic BW, the mass (adding J/ψ mass) and width of this structure, including systematic uncertainties, are measured to be $4143.0 \pm 2.9(\text{stat}) \pm 1.2(\text{syst})$ MeV/c^2 and $11.7^{+8.3}_{-5.0}(\text{stat}) \pm 3.7(\text{syst})$ MeV/c^2, respectively. This structure does not fit conventional expectations for a charmonium state because as a $c\bar{c}$ state it is expected to have a tiny branching ratio to $J/\psi\phi$ with its mass well beyond open charm pairs. We term the new structure the $Y(4140)$. The branching ratio of $B^+ \rightarrow Y(4140)K^+, Y(4140) \rightarrow J/\psi\phi$ is estimated to be $9.0 \pm 3.4(stat) \pm 2.9(B_{BF})) \times 10^{-6}$.

ACKNOWLEDGMENTS

REFERENCES

1. M. Kramer, arXiv:hep-ph/0106120.
2. T. Afolder *et al.,* (CDFCollaboration), Phys. Rev. Lett. **85**, 2886 (2000); T. Abulencia *et al.,* (CDFCollaboration), Phys. Rev. Lett. **99**, 132001 (2007).
3. http://www-cdf.fnal.gov/physics/new/bottom/090903.blessed-Upsilon1S-polarization/blessed_plots.html.
4. V. Abazov, *et al.,* (D0 Collaboration), Phys. Rev. Lett. **101**, 012001 (2008).
5. D. Acosta, *et al.*, (CDFCollaboration), Phys. Rev. Lett. **88**, 161802 (2002).

6. S.-K. Choi *et al.* (Belle Collaboration), Phys. Rev. Lett. **91**, 262001 (2003); D. Acosta *et al.* (CDF Collaboration), Phys. Rev. Lett. **93**, 072001 (2004); S.-K. Choi *et al.* (Belle Collaboration), Phys. Rev. Lett. **94**, 182002 (2005); B. Aubert *et al.* (*BABAR* Collaboration), Phys. Rev. Lett. **95**, 142001 (2005); S. Godfrey and S. L. Olsen, Ann. Rev. Nucl. Part. Sci **58** (2008) 51.

7. S.-K. Choi *et al.* (Belle Collaboration), Phys. Rev. Lett. **94**, 182002 (2005); B. Aubert *et al.* (*BABAR* Collaboration), Phys. Rev. Lett. **101**, 082001 (2008).

8. B. Aubert *et al.* (*BABAR* Collaboration), Phys. Rev. Lett. **95**, 142001 (2005).

9. B. Aubert *et al.* (*BABAR* Collaboration), Phys. Rev. Lett. **98**, 212001 (2007); X. L. Wang *et al.* (Belle Collaboration), Phys. Rev. Lett. **99**, 142002 (2007); S.-K. Choi *et al.* (Belle Collaboration), Phys. Rev. Lett. **100**, 142001 (2008); R. Mizuk *et al.* (Belle Collaboration), Phys. Rev. D **78**, 072004 (2008); P. Pakhlov *et al.* (Belle Collaboration), Phys. Rev. Lett. **100**, 202001 (2008).

10. E. Eichten, S. Godfrey, H. Mahlke, and J. Rosner, Rev. Mod. Phys. **80**, 1161 (2008); S. L. Zhu, Phys. Lett. B **625**, 212 (2005); F. Close and P. Page, Phys. Lett. B **628**, 215 (2005); E. S. Swanson, Phys. Lett. B **588**, 189 (2004); L. Maiani, F. Piccinini, A. D. Polosa, and V. Riquer, Phys. Rev. D **72**, 031502(R) (2005); N. V. Drenska, R. Faccini, and A. D. Polosa, arXiv:hep-ph/0902.2803v1. T. W. Chiu and T. H. Hsieh, Phys. Lett. B **646**, 95 (2007).

11. C. Amsler *et al.* (Particle Data Group), Phys. Lett. B **667**, 1 (2008).

12. T. Aaltonen *et al.* CDF Collaboration, arXiv:0906.5218 [hep-ex];

13. I. Adachi, *et al.* (Belle Collaboration), arXiv:0809.1224v1 [hep-ex].

14. T. Aaltonen *et al.* CDF Collaboration, Phys. Rev. Lett. **102**, 242002 (2009).

15. B. Aubert *et al.* (*BABAR* Collaboration), Phys. Rev. D **78**, 071103 (2008).

16. $\frac{dN}{dm} \propto \frac{m\Gamma(m)}{(m^2-m_0^2)^2+m_0^2\Gamma^2(m)}$, where $\Gamma(m) = \Gamma_0 \frac{q}{q_0} \frac{m_0}{m}$, and the 0 subscript indicates the value at the peak mass.